

Global projections of storm surges using high-resolution CMIP6 climate models: validation, projected changes, and methodological challenges

Sanne Muis^{1,2}, Jeroen C. J. H. Aerts^{1,2}, José A. Á. Antolínez³, Job C. Dullaart², Trang Minh Duong^{1, 4, 5}, Li Erikson⁶, Rein J. Haarsma⁷, Maialen Irazoqui Apecechea^{1,8}, Matthias Mengel⁹, Dewi le Bars⁹, Andrea O'Neill⁶, Roshanka Ranasinghe^{1,4,5}, Malcolm J. Roberts¹⁰, Martin Verlaan^{1,3}, Philip J. Ward², Kun Yan¹

1. Deltares, Delft, The Netherlands
2. Vrije Universiteit Amsterdam, Amsterdam, The Netherlands
3. TU Delft, Delft, The Netherlands
4. IHE Delft Institute for Water Education, Delft, The Netherlands
5. University of Twente, Enschede, The Netherlands
6. USGS, Santa Cruz, USA
7. KNMI, De Bilt, The Netherlands
8. Mercator Ocean, Toulouse, France
9. Potsdam Institute for Climate Impact Research, Potsdam, Germany
10. Met Office Hadley Centre, Exeter, UK

Corresponding author: Sanne Muis (sanne.muis@vu.nl)

Key points:

1. New global projections of extreme sea levels by forcing the Global Tide and Surge Model with a ~25km-resolution climate models ensemble
2. Validation against ERA5 shows that the 1 in 10-year surge levels have a good overall performance, but there is a large-scale spatial bias
3. Comparison of 2021-2050 against 1951-1980 shows that the 10-year storm surges may increase or decrease up to 0.1 m or 20% over this period

Abstract

In the coming decades, the frequency of coastal flooding will increase due to sea-level rise and changes in climate extremes. We force the Global Tide and Surge Model (GTSM) with a climate model ensemble from the CMIP6 High Resolution Model Intercomparison Project (HighResMIP) to produce global projections of extreme sea levels (defined as tides and storm surge) from 1950 to 2050. This is the first time that an ensemble of global ~25km resolution climate models is used

for this purpose, which increases the credibility of projected storm surges. Here we validate the historical simulations (1985-2014) against the ERA5 climate reanalysis. The overall performance of the HighResMIP ensemble is good with mean bias smaller than 0.1 m. However, there is a strong large-scale spatial bias. Future projections for the high emission SSP5-8.5 scenario indicate changes up to 0.1 m or 20% in 10-year return period surge level from 1951-1980 to 2021-2050. Increases are seen in parts of the coastline of the Caribbean, Madagascar and Mozambique, Alaska, and northern Australia, whereas the Mediterranean region may see a decrease. The full dataset underlying this analysis, including timeseries and statistics, is openly available on the Climate Data Store and can be used to inform broad-scale assessment of coastal impacts under future climate change.

Introduction

Extreme sea levels (ESL), composed of mean sea level variations, tides, storm surges and waves, can cause coastal flooding and erosion. This can lead to severe damages to the livelihoods of people, economic assets, and coastal ecosystems. According to the Sixth Assessment Report (AR6) of the Intergovernmental Panel on Climate Change (IPCC), by 2100 global mean sea level may be up to 1m higher than 1995-2014 in the SSP5-8.5 scenario of high energy demand and high fossil fuel dependence (Fox-Kemper et al., 2021). The rise in mean sea level will drive steep increases in ESL frequencies (Frederikse et al., 2020; Vousdoukas et al., 2018). Even if global warming is limited to 1.5°C above pre-industrial levels, a target agreed upon in the Paris Agreement, about half of the world’s coastline will experience the present-day 100-yr ESL at least once a year by 2080 (Tebaldi et al., 2021). Besides higher mean sea levels, the warming of the climate and change in the large-scale atmospheric circulation can modulate the occurrence of tropical cyclones and extra-tropical storms. The change in ESL frequencies depends on the combined effect of changes in storm intensity and tracks. While the total number of tropical cyclones may decrease or remain unchanged (Sobel et al., 2021), tropical cyclone intensities are projected to increase in response to warmer sea surface temperatures (Knutson et al., 2010, 2019, 2020; Walsh et al., 2016). Most projections show an increase in the proportion of intense tropical cyclones (category 4-5) and higher maximum wind speeds (Knutson et al., 2020). Moreover, in a warmer climate, tropical cyclone tracks will shift poleward (Haarsma, 2021; Haarsma et al., 2013). Future projections of changes for storms in the mid-latitude regions are generally small, although some regions may see substantial changes due to a poleward shift in the extra-tropical storm tracks (Seneviratne et al., 2021). Many studies have explored how storm surge frequencies may change in a warmer climate, often at regional to country scale (Colberg et al., 2019; Garner et al., 2017; Lin et al., 2019; Little et al., 2015; Marsooli et al., 2019), but more recently also at the continental to global scale (Mori et al., 2019; Muis et al., 2020; Vousdoukas et al., 2016, 2018).

Global ESL models have evolved rapidly in recent years, and now include more physical processes at increasing resolution (Bouwer, 2018; Wahl, 2017). This has led to an enhanced understanding of extreme sea levels and associated coastal flooding (Muis et al., 2016), and how flood hazard and risks may be impacted by climate change and adaptation (Kirezci et al., 2020; Mori et al., 2019; Tiggeoven et al., 2020; Vitousek et al., 2017; Vousdoukas et al., 2018). Mean sea level will be the largest driver of changes in ESL (Vousdoukas et al., 2018), and most global studies have projected future changes in ESL resulting from mean sea level changes (Frederikse et al., 2020; Kirezci et al., 2020; Rasmussen et al., 2018; Tebaldi et al., 2021; Vitousek et al., 2017). This approach neglects the high potential but not yet fully understood contribution from changes in tropical cyclones and extratropical storms (Seneviratne et al., 2021). Studies that have provided global to continental-scale projections of storm surges are based on Global Climate Models (GCMs) from the Coupled Model Intercomparison Project - Phase 5 (*CMIP5*) experiments (Colberg et al., 2019; Lin et al., 2019; Muis et al., 2020; Vousdoukas et al., 2018). A major limitation of the *CMIP5* experiments is that the GCM’s spatial resolution (~ 150 km) is insufficient to resolve localized climate extremes, such as tropical cyclones (Camargo, 2013; Hodges et al., 2017; Schenkel & Hart, 2012). With further GCM development and increases in resolution (Bauer et al., 2015), there is a growing number of GCMs that can generate a credible climatology of both TC numbers and intensities in the current climate (Murakami et al., 2012; M. J. Roberts et al., 2020; Walsh et al., 2016). The High Resolution Model Intercomparison Project (High-ResMIP) which is part of the *CMIP6* framework, provides climate projections of models with a spatial resolution up to 25-50 km (Haarsma et al., 2016). This means that for the first time it is possible to derive credible global projections of ESL, including changes in storm surges.

Here we present global ESL projections that are derived from an ensemble of high-resolution climate models. While the full datasets includes total water levels, tides and storm surges, the analysis presented here focusses on the 10-year storm surge level. First, we evaluate the performance of the ensemble for the historical period against the ERA5 reanalysis in terms of surge levels. Next, we assess projected future changes in surge levels. Finally, we discuss remaining methodological challenges and directions for future research.

Methods & Data

Figure 1 summarizes the three-step methodology that was used to generate the global storm surge projections. First, we derive timeseries of total water levels, tides and surge levels by forcing the Global Tide & Surge Model (GTSMv3.0) with sea level pressure and wind speed from an ensemble of HighResMIP models. Second, we split the timeseries into three periods (1951-1980, 2014-1985 and 2021-2050) and perform extreme value analysis. Next, we quantify how the magnitude and frequency of storm surges may be impacted by future climate

change. Below each of the steps is explained in more detail.

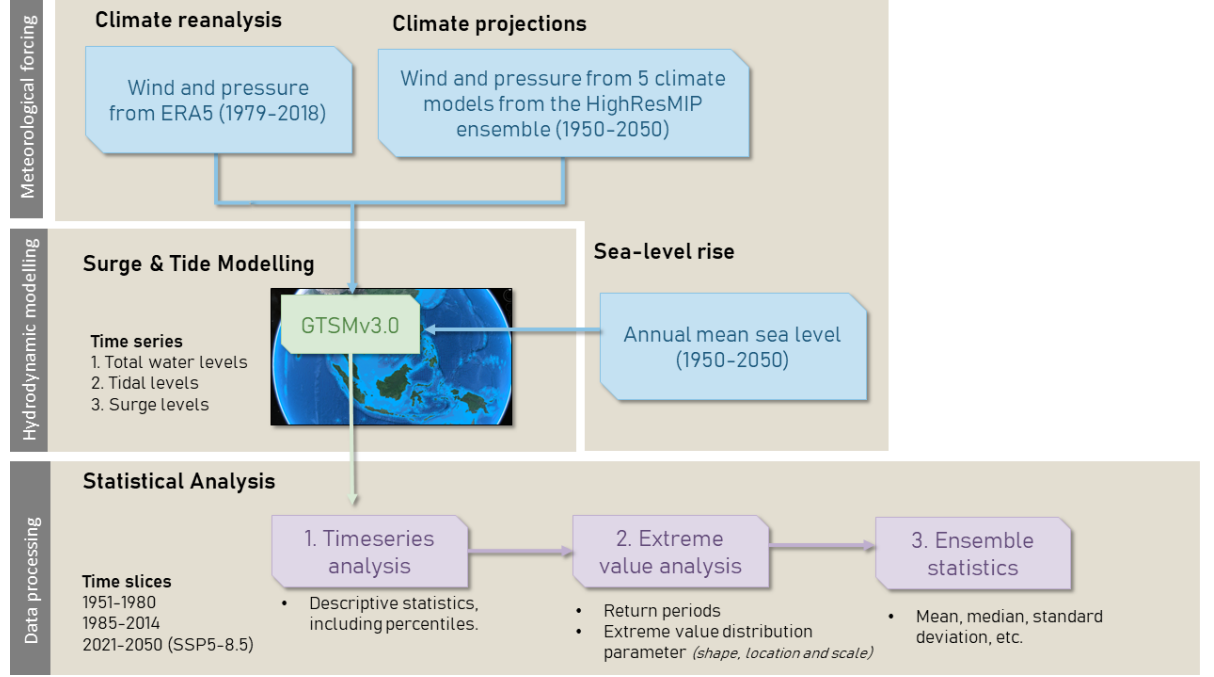


Figure 1 Flowchart of the modelling approach that was used to generate the global projections of extreme sea levels.

Global modelling of storm surges

We use the third-generation Global Tide and Surge Model (GTSMv3.0) to simulate total water levels resulting from tidal and meteorological forcing (Muis et al., 2020; Wang et al., 2021). GTSM is a depth-averaged hydrodynamic model based on the Delft3D Flexible Mesh modelling suite (Kernkamp et al., 2011). The grid resolution ranges from 2.5 km along the coast (1.25 km in Europe) to 25 km in the ocean. Non-linear interactions between tides, storm surges and mean sea levels are dynamically included. We obtain time series of storm surges by computing the difference between a tide-only run and a total water level simulation. There are no open boundaries and tides are modelled by including tide generating forces (i.e. the gravitational attraction and centrifugal forces of the Earth, Moon, and Sun) using a set of 60 tidal frequencies. For the total water level simulation, GTSM is forced with 10 m wind speed and sea level pressure from the climate models and tidal forcing. The tide-only simulation excludes meteorological forcing. For both simulations, we include a spatially-varying sea-level rise field based on CMIP5 models for the entire simulation period (Text S1 and Figure S1). Time series at 10-minute resolution are produced for a set of 43,119 output points (Muis et al., 2020). GTSM has been extensively validated

in previous studies (Bloemendaal et al., 2017; Dullaart et al., 2020; Irazoqui Apecechea et al., 2019; Muis et al., 2016, 2019, 2020), which have shown good agreement between modelled and observed water levels.

HighResMIP climate projections

To analyse the changes in storm surges under climate change, we force GTSM with meteorological fields of the multi-model HighResMIP ensemble (Haarsma et al., 2016), which consists of five ~ 25 km resolution Global Climate Models (GCMs). The HighResMIP experiments span the period 1950–2050. For the historic simulations (1950–2014), the forcing fields are similar to those used in CMIP6 historic simulations (Eyring et al., 2016), although at higher resolution. The future simulations (2015–2050) in our study are based on the SSP5-8.5 greenhouse gas concentration scenario (O’Neill et al., 2016). We use a mix of coupled atmosphere-ocean and atmosphere-only simulations; specifically, three coupled simulations [HadGEM3-GC31-HM (Roberts, 2017), Earth3P-HR (EC-Earth Consortium, 2018), CMCC-CM2-VHR4 (Scoccimarro et al., 2017)] and two atmosphere-only simulations [HadGEM3-GC31-HM-SST (Roberts, 2017), GFDL-CM4C192-SST (Zhao et al., 2018)]. The atmosphere-only simulations have prescribed daily sea-surface temperature (SST) fields. Ideally, we would have used a larger model ensemble based on coupled simulations only. However, at the time of carrying out the GTSM simulations these were the only simulations available with a minimum temporal resolution of at least 6 hours. For validation of the HighResMIP ensemble, we also force GTSM with the ERA5 climate reanalysis from 1979 to 2018 (Copernicus Climate Change Service (C3S), 2017; Hersbach et al., 2020). ERA5 is the successor of ERA-Interim and has hourly fields with a spatial resolution of $0.25^\circ \times 0.25^\circ$ (~ 31 km at the equator).

Data processing and statistical analyses

We split the storm surge time series into three periods: 1951–1980, 1986–2014 and 2021–2050. Subsequently, we compute descriptive statistics at each output location for each of these three time slices. The descriptive statistics computed are: mean, standard deviation, skewness, kurtosis, and percentiles (1, 5, 10, 25, 50, 75, 90, 95, 99, 99.5, 99.9). In addition, we apply extreme value analysis (EVA) to estimate the exceedance probabilities of surge levels. Following Wahl et al. (2017), we follow the Peak Over Threshold method (POT) and we fit the Generalized Pareto Distribution (GPD) on the peaks that exceed the 99th percentile surge level, then we derive estimates for various return periods. We ensure independence between storm events by using a 72h period for the de-clustering of the peaks (Vousdoukas et al., 2018). We apply bootstrapping with 599 repetitions for the parameter estimates to assess the 5% and 95% confidence intervals (Wilcox, 2010). Because our data have a 10-minute temporal resolution, we define a minimum storm duration (defined as the time above the threshold) of 60 minutes to skip erroneous individual data points. We use the Maximum Likelihood Estimation (MLE) to fit the GPD parameters, and we set

a starting estimate of zero for the shape parameter. Extreme value distributions other than GPD were also fitted. This includes the Exponential distribution following POT method, and Gumbel and Generalized Extreme Value distribution following annual maxima method. This shows that the return period estimates provided by GPD are robust for the 10-year return levels that we analyse here.

We first evaluate the performance of the HighResMIP ensemble by comparing the return periods and the percentiles derived from the HighResMIP simulations against those derived from the ERA5 simulation for the period 1985-2014 (section 3.1). The computed performance metrics include Pearson’s correlation coefficient, mean bias (m), and the mean relative bias (%). To assess the influence of climate change over, we analyse the changes in 1 in 10-year storm surges by comparing the return periods of 1985-2014 and 2021-2050 against the reference period 1951-1980 (section 3.2). Changes are computed for each individual HighResMIP model, as well as the median change across the multi-model ensemble. With such a small ensemble, the mean is easily distorted by outliers; for this reason, we focus on the median values. Moreover, to minimize the uncertainty of the extreme value fit, we focus on the 10-year return period rather than the 100-year return period. We assess the inter-model spread by computing the standard deviation of the projected changes across the different climate models. We also assess the inter-model agreement on the sign of change by computing the number of ensemble members indicating a increase or decrease in the return period values. For both the validation and analysis of changes, we use the reference regions of the IPCC AR6 report (Iturbide et al., 2020) to evaluate regional differences.

Results and discussion

Validation of storm surges based on the historical simulations

Figure 2a displays a global map of the 10-year return period for storm surges for the period 1985-2014, showing the median of the 5-member model ensemble. There are high values in coastal areas with a shallow continental shelf and a stormy climate, whereas low values are seen in equatorial areas with a steep ocean topography. Low values also occur on the southern Gulf Coast (U.S. and Mexico), near Mozambique and Madagascar, and some other regions where low-probability tropical cyclones are the main driver of extremes (see Dullaart, 2020). Regions with return levels exceeding 2.0 m include the North Sea (Northwest Europe), Hudson Bay (Canada), Gulf of Carpentaria (North Australia), Patagonia (Argentina), and the Yellow Sea (China). These are also the regions where the spread of the ensemble is largest, as indicated by the standard deviation in Figure 2b. This in contrast with regions with small storm surges where the spread is low.

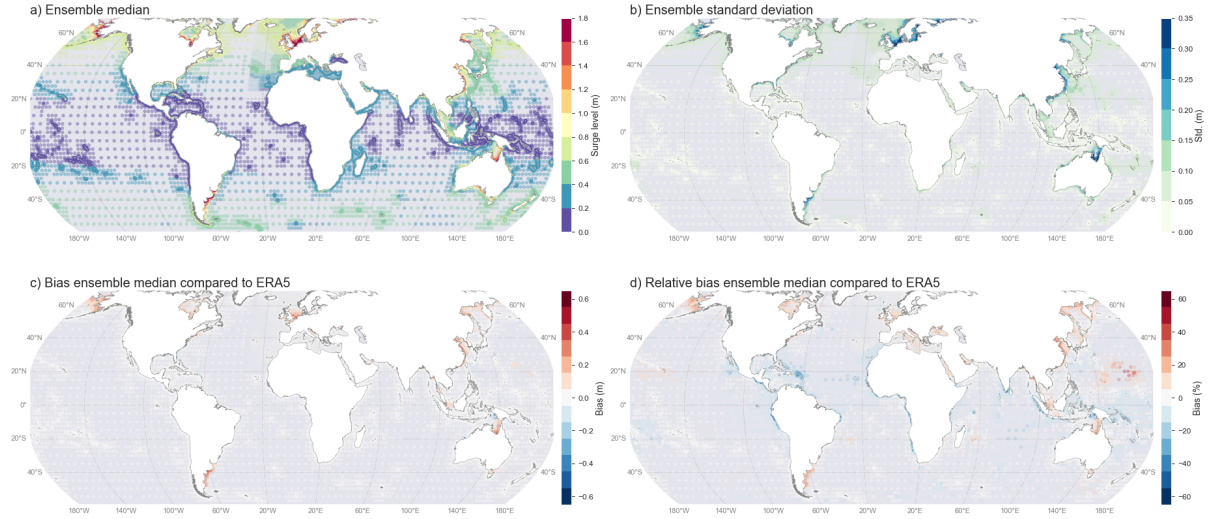


Figure 2 Global map of storm surge levels with a 10-year return period. Panel **a** shows the median of the HighResMIP ensemble for period 1985–2014, while panel **b** shows the standard deviations. Panel **c** and **d** show, respectively, the bias (m) and the relative bias (%) of multi-model median in comparison with the ERA5 reanalysis for the same period.

To evaluate how well the HighResMIP ensemble performs, we compare the 1, 10 and 100-year return period against return periods derived from the ERA5 reanalysis using the same methods. Table 1 summarizes the performance for the ensemble median and the individual models. The multi-model median shows a better overall agreement with ERA5 than the individual ensemble members. In general, the large-scale spatial pattern is well-captured as indicated by high correlation coefficients ($r > 0.9$). The height of storms surges and its large-scale spatial pattern is influenced by the (accuracy of the) meteorological forcing, but also by the bathymetry. The HighResMIP and ERA5 simulations both use the same model configuration (such model grid and bathymetry), and the high correlation coefficient reflect this. Averaged across all output locations, the model bias is small ($< 0.1\text{m}$). This indicates that compared to ERA5 the HighResMIP ensembles performs well. However, Figures 2b and c show that the ensemble median has a clear spatial bias, with mostly negative values at the tropics and positive values at mid- to high-latitude areas. The overestimation compared to ERA5 is most profound in areas with a wide coastal shelf, such as the Yellow Sea (China), Gulf of Carpentaria (North Australia), and the North Sea (North-western Europe). Figure 3 shows the relative bias for the 1 in 10-year surge level, aggregated into the IPCC reference regions. This clearly shows the spatial coherency of the bias. This pattern is consistent for the 1, 10 and 100-year return periods, which suggests that there is a systematic bias in the HighResMIP ensemble that propagates into the extreme value analysis. This is confirmed by mapping the bias for the 75th, 90th, and 95th percentiles of the

surge level timeseries (Figure S2), which show a similar spatial bias. We argue the part of the bias that is already present for normal climate conditions is caused by systematic errors in the large-scale atmospheric circulation. The bias for more extreme climate conditions is depending on the accurate representation of storm frequency, intensity and track.

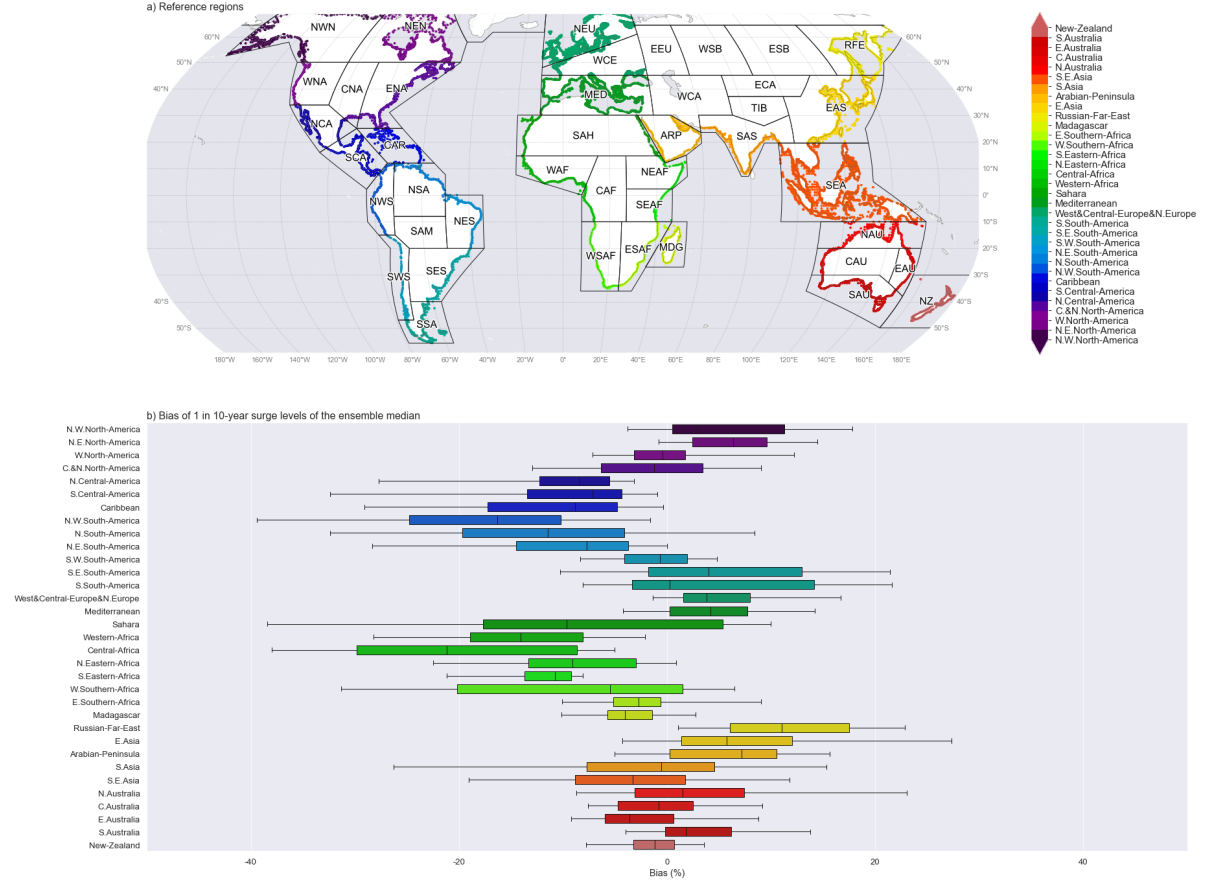


Figure 3 Bias of in the 1 in 10-year surge level (m) between the HighResMIP ensemble median and ERA5, aggregated into the IPCC reference regions. Panel **a** shows the regions with the colours corresponding to the colours of the boxplots in panel **b**. The extent of each box shows the interquartile range across locations within the region (25th-75th percentile), the vertical black line indicates the median value (50th percentile) and the extent of the whiskers indicates the range of the 5-95th percentiles. The separate dots indicate outliers. Note that not all outliers are displayed because of the axis's limits and visibility.

There are notable differences in the performance of the different HighResMIP models for the different return periods. The EC-Earth3P-HR and HadGEM3-GC31-HM have a comparable and relatively good performance, which is stable

across the different return periods (Table 1). The performance of HadGEM3-GC31-HM-SST with fixed sea surface temperatures is worse than for the respective coupled simulation, with the doubling of mean bias from 5% to 10% for the 10-year return period surge level. While the atmosphere-only simulation may be less affected by a bias in SST, this may be counteracted by the fact that atmosphere-ocean coupling may results in a more realistic representation of extreme winds. The mean bias of CMCC-CM2-VHR4 is higher than for the other models, especially for the 100-year return period with a 0.14 m bias. GFDL-CM4C192-SST has a negative mean bias, which is most profound for the low return periods. Although the magnitude differs, most of the individual HighResMIP models also show a clear spatial bias (Figure S3). Similarly, as for the ensemble median, this bias is not just caused by deficiencies in the extremes. For example, in GFDL-CM4C192-SST the normal climate conditions already introduce a negative bias, while extremes seem to be overestimated.

	Return period (yrs)	EC-Earth3P-HR	HadGEM3-GC31-HM	HadGEM3
Pearson correlation coefficient	1	0.989	0.987	0.987
	10	0.981	0.980	0.978
	100	0.888	0.905	0.850
Relative Bias (m)	1	0.01 (0.07)	0.04 (0.08)	0.06 (0.09)
	10	0.02 (0.14)	0.06 (0.13)	0.10 (0.16)
	100	0.03 (0.39)	0.07 (0.35)	0.14 (0.48)
Mean Relative Bias (%)	1	-2.39 (12.5)	5.04 (12.8)	10.2 (11.3)
	10	-1.38 (15.3)	5.39 (14.6)	12.1 (15.2)
	100	-0.58 (24.5)	5.85 (19.4)	14.7 (47.4)

Table 1 Model performance of the HighResMIP ensemble for surge levels with a return period of 1, 10 and 100 years. The HighResMIP ensemble is compared against surge levels derived with the ERA5 reanalysis. Values are averaged across all output locations with the standard deviation in brackets.

Changes in storm surges for the HighResMIP ensemble

Next, we analyse the changes in surge levels for the periods 1985-2014 and 2021-2050 (SSP5-8.5), relative to 1951-1980 (the reference period). Figure 2a-b shows that for most of the world’s coastline, the changes for 1985-2014 in surge level are small. For 90% of the output locations, the relative changes are generally lower than 5% and absolute changes are smaller than 0.1 m from 1985-2014 to 2021-2050. The largest increases in the 10-year return period for this time slice occur in the southern part of the North Sea, the Gulf of Carpentaria (Australia), the Bering Sea (Russia and Alaska), and the South China Sea (Vietnam and China), while the largest decreases occur near the Gulf of St. Lawrence (Quebec, Canada) and the Yellow Sea (Northeast China and North- and South Korea). For the future period 2021-2050, the projected changes in surge levels under

SSP5-8.5 are often larger. For about 25% of the coastal output locations the median change in 1 in 10-year return is larger than 5% from 2021-2050 to 1951-1980. Compared to 1985-2014 the change signal for the Bering Sea and Gulf of Carpentaria becomes more coherent, while for the North Sea and South China Sea the signal becomes more scattered. The largest decreases occur in the Mediterranean Sea and the Australian Bight. For some of the other regions the sign of change flips when comparing the projected changes between 1985-2014 and 2021-250 against 1951-1980s. This indicates that surge-level trends from 1950 to 2050 are not always linear. A potential reason can be that the natural climate variability affects the 1 in 10-year return period surge events in our analysis that is based on time periods of 30 years only.

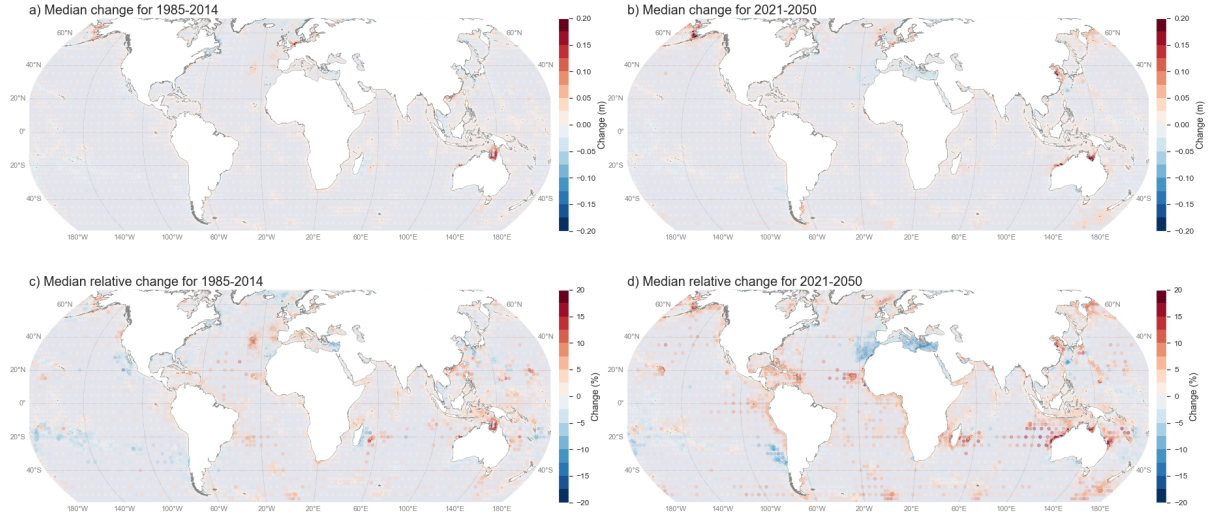


Figure 4 Ensemble-median absolute (panels a and b) and relative (panels c and d) changes in the 10-year surge levels for the periods 1985-2014 and 2021-2050, using 1951-1980 as reference period.

Next, we analyse the projected change in the 1 in 10-year surge levels across the ensemble, aggregated to the IPCC-AR6 reference regions (Figure 5). Generally, across larger spatial scales the surge-level changes tend to cancel each other out as most regions see both increases and decreases. At local scale the projected changes may be larger, but when aggregated to regional scale the median change is around zero and the interquartile (25th to 75th percentile) range of the changes is within 0.05 m for almost all regions. An expectation is for North and Central Australia where the interquartile range reaches up to an increase in surge level of 0.1 m. Generally, the distribution of the changes is asymmetrical with 26 of the 32 regions having a distribution that is highly skewed towards increases in surge. The changes for the future period are larger than for the current period in all regions.

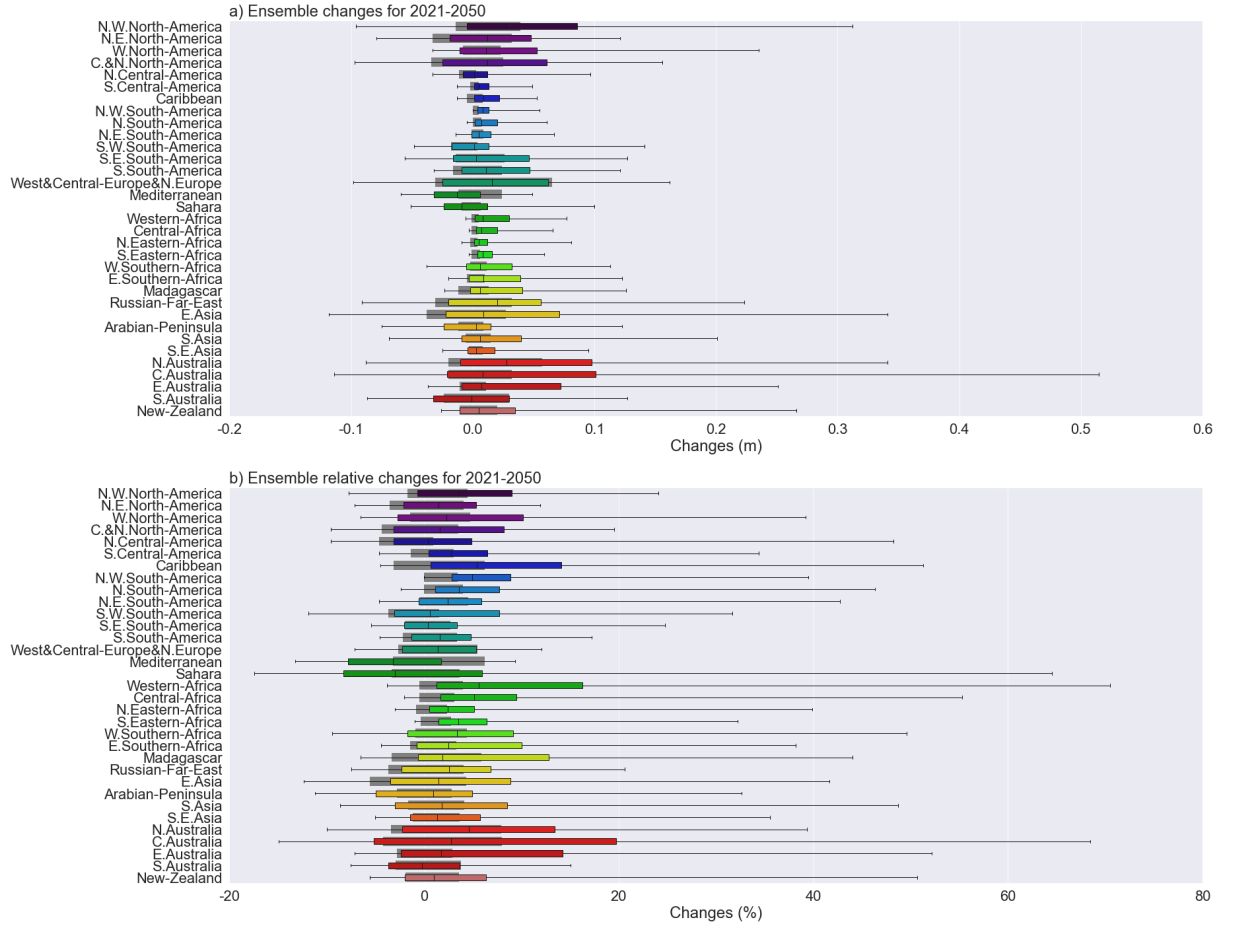


Figure 5 Statistics of projected changes in the 1 in 10-year surge level between 2021-2050 with 1951-1980 as reference, aggregated into the IPCC-AR6 regions. The coloured boxes show the interquartile range (25th-75th percentile) across locations within the region, the vertical black line indicates the median value (50th percentile) and the extent of the whiskers indicates the range of the 5-95th percentiles. The colour of the bars is corresponding with the map in Figure 3a. The grey boxes show the interquartile range of changes between the 1985-2014 and 1951-1980. The projected changes computed based on the individual HighResMIP models (and not the ensemble median).

The HighResMIP ensemble has considerable intermodel variability with the several models projecting different changes. Whilst the ensemble only contains 5 models, we quantify the consistency of the ensemble by showing the intermodel agreement on the sign of change. Figure 6a and b display the number of models that project an increase or decrease in the 1 in 10-year surge levels for the periods 1985-2014 and 2021-2050, relative to 1951-1980. We find that there are only

a few places where there is a clear majority of the models (more than 3) agrees on the sign of change. This in part may be due to natural variability. However, the changes relative to 1951-1980 are more consistent across the ensemble for the future period 2021-2050 under SSP5-8.5 than for the period 1985-2014. The changes also have a larger spatial coherency. Regions where the ensemble consistently shows an increase in the 1 in 10-year surge level include parts of the North Sea (Northwest Europe), Yellow Sea (Eastern China), Patagonia, and northern Australia. For the southern part of the Mediterranean the models agree on a decrease. For many other regions, such as the Persian Gulf (Saudi Arabi, Iran) and the Gulf Coast (southern United States and Mexico) there is no clear majority. Figure 6c and d shows the intermodel spread expressed as the standard deviation of the changes across the ensemble. As expected from the larger magnitude of changes, the spread is generally large in areas with high storm surges, like the North Sea and Gulf of Thailand. While having higher consistency, for the period 2021-2050 the intermodel spread is larger than for the period 1985-2014. Figure S4 shows the projected changes of the individual members of the HighResMIP ensemble.

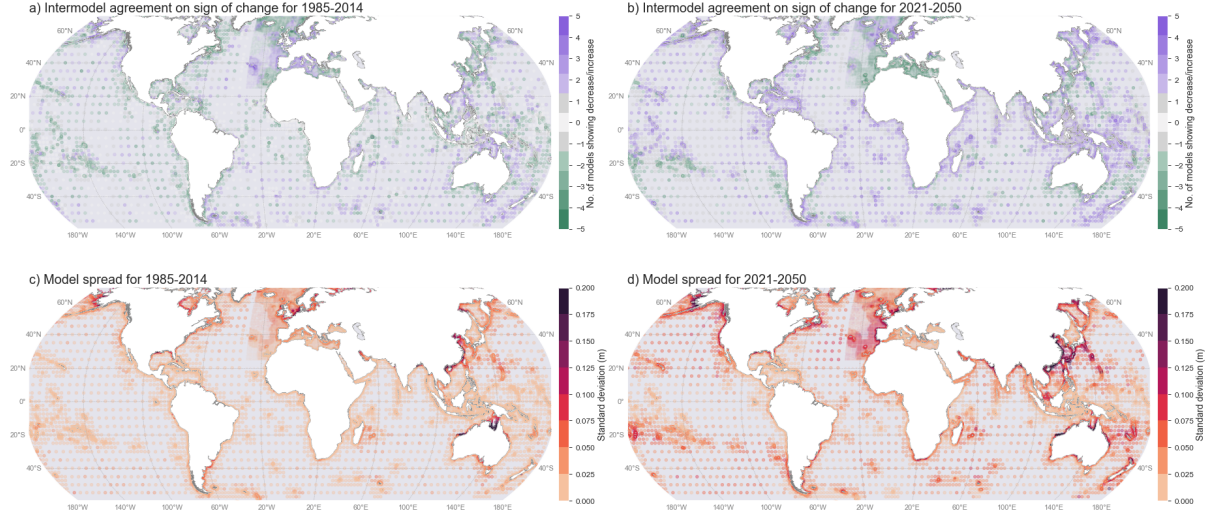


Figure 6 Robustness of the projected changes across the model ensemble for 1 in 10-year surge levels with the intermodel agreement (panel a and b) as expressed by the number of models agreeing upon the sign of change, and the model spread (panel c and d) as expressed by the standard deviation. We show the changes for the periods 1985-2014 and 2021-2050, using 1951-1980 as reference period.

Methodological challenges and ways forward

Limitations of modelling approach

The key component of our approach is GTSMv3.0, which is a depth-averaged barotropic model. GTSM is designed specifically for the global modelling of tides and storm surges with high accuracy in coastal areas. In regions with a steep topography, such as oceanic islands, ESLs are not primarily caused by storm surges but driven by wind-driven waves sometimes in combination with mean sea level variations (Woodworth et al., 2019). Wind-driven waves can co-occur with storm surges (Marcos et al., 2019), and for future research it would be valuable to develop wind-wave projections based on the same climate model ensemble, and analyse the combined effects of waves and storm surges on the frequency of coastal flooding (Kirezci et al., 2020; Vousdoukas et al., 2018). Our methodology is based on annually updated mean sea levels. As such, we exclude seasonal and intra-annual variation in mean sea level that are not captured by GTSM, for example those driven by density changes or river inflows. Moreover, we have used the same mean sea level fields for all simulations. These fields are derived by averaging over the CMIP5 models and based on our best guess for Antarctica. However, both sea-level rise and changes in tropical cyclones are steered by thermodynamic and dynamic climate changes, and are therefore positively correlated. Lockwood et al. (2022) have shown that considering SLR and TC changes independently may not accurately represent future ESL changes. One aspect of our approach that could be improved is the coupling of the hydrodynamic model with the climate models. We use a constant value for the wind drag based on Charnock (1955), although the efficiency of the air-sea momentum transfer will depend on the sea state and the wind speed (Powell et al., 2003; Ridder et al., 2018). The implementation of a spatially and temporally varying wind drag parameterization in GTSM should be the focus of future work. For ERA5 it is well-documented to what exact formulations are used for the sea-air momentum transfer, which makes implementation relatively straightforward. However, this is not the case for the HighResMIP models, and climate model simulations in general.

Biases of the HighResMIP ensemble

From other climate impact studies, such as wave and hydrological modelling (Lemos et al., 2020; Navarro-Racines et al., 2020), it is well-known that GCMs can have severe biases in representing extremes. Previous global studies have given little attention to assessing and resolving systematic biases for storm surge modelling. Our results highlight that, moving forward, we need to investigate in greater depth what causes the deviations between ERA5 and the HighResMIP models. It can be expected that previous global projections derived with coarser resolution CMIP5 models, such as Muis et al., (2020) and Vousdoukas et al., (2018), have similar if not larger spatial biases. While it may be challenging, the attribution of the systematic bias to underlying causes is important. For

instance, the bias can stem from too low or too high numbers of extreme events as well as an over- or underestimation of the magnitude of the extremes. For the HighResMIP ensemble it has been shown that TC frequencies are comparable to observations, and that increased horizontal resolution improves the representation of TC intensity and tracks, although the strongest TCs may still be underestimated (Roberts et al., 2020). In terms of extra-tropical storms, Priestley et al. (2022) have shown that for the CMIP6 models, biases in the sea surface temperature play an important role in the introduction of biases in storm tracks in the Northern Hemisphere, and suggest that the atmosphere-only simulations perform better in these areas. The 25-km resolution of the HighResMIP models should be beneficial for representation of extremes. At the same time, the increases resolution of the HighResMIP ensemble may result in higher climate sensitivity and enhanced variability, and this may be one of the reasons for deviations from ERA5. The large-scale bias is visible for lower percentiles indicating that the bias cannot be fully attributed to the representation of extremes, and suggesting that biases in the large-scale atmospheric circulation also play a role. We minimize the effect of the bias by only reporting changes between the different periods simulated by that same GCM. Although bias correction cannot address fundamental problems of GCMs, methods such as the so-called delta-change method are commonly applied (Eisner et al., 2012; Hemer et al., 2013; Morim et al., 2019). In future research, more advanced bias correction methods such as quantile mapping (Lemos et al., 2020; Tebaldi & Knutti, 2007), could be applied to further reduce the bias. The impact of the bias could be further reduced by putting less weight on models that have a large bias in a specific region (Marsooli et al., 2019).

Enhancing the confidence in projected changes

The IPCC’s Sixth Assessment Report notes that “Quantifying the effect of climate change on extreme storms is challenging, partly because extreme storms are rare, short-lived, and local, and individual events are largely influenced by stochastic variability” (Seneviratne et al., 2021). We have presented new global ESL projections that are derived with a multi-model ensemble of ~25 km resolution GCMs from HighResMIP, as part of CMIP6. There are, however, quite a few remaining methodological challenges. We believe that there are several ways forward, which we outline below. First, an essential first step in improving the reliability of the projections is addressing the spatial bias. As explained above, we need to invest in efforts to better understand the causes of these biases and subsequently design methods to reduce them. Second, ERA5 will be extended back to 1950. This would make it possible to validate the projected changes from 1951-1980 to 1985-2014, and see if the results for the HighResMIP simulations are consistent with the climate reanalysis. Third, while computationally expensive, extending our ensemble with more models would be valuable, and would add robustness to subsequent statistical analyses. Currently our ensemble consists of a mix of 5 coupled and atmosphere-only simulations. The heterogeneity and the small number of ensemble members make it difficult to

say much with statistical uncertainty. Very recently, a few more HighResMIP models have become available, and a larger ensemble would allow better quantification of intermodel agreement (percentage of models that agrees on sign of change, etc). Moreover, some of the HighResMIP models have multiple members, which could be useful to quantify internal climate variability. This would help in disentangling the signal of anthropogenic-forced climate change from the internal climate variability. The quantification of internal variability is not possible in the 5-member ensemble of this study, and could be one of causes for the intermodel disagreement. Fourth and last, extreme value analysis is generally associated with large uncertainties (Wahl et al., 2017). The small sample size is especially problematic for regions prone to tropical cyclones, which have low probabilities that cannot be adequately assessed with time slices of 30 years. A robust assessment of changes for those regions would require stochastic modelling of events representing thousands of years of tropical cyclone activity (Dullaart et al., 2021; Haigh et al., 2013; Lin & Emanuel, 2015; Marsooli et al., 2019; Orton et al., 2016). Also for extra-tropical regions internal climate variability may be a significant influence. Calafat et al. (2022) have provided observational evidence that, in Europe, climate variability can considerably affect the probabilities of surge extremes over periods as long as 60 years suggesting that 30-year time slices may not be long enough for a robust estimation of even the 10 year return period surge level. An alternative approach would be to consider the HighResMIP models as independent realizations of climate extremes and apply the “pooled” ensemble approach described by Meucci et al. (2020).

Conclusions

Using the CMIP6 HighResMIP climate model simulations, we have developed global multi-model projections of extreme sea levels (ESLs) from 1950 to 2050. The ~25 km resolution of the CMIP6 HighResMIP ensemble represents a step-change compared to the previous coarse resolution CMIP5-based simulations that fail to fully capture climate extremes such as tropical cyclones. Comparison of the ESLs derived from HighResMIP ensemble against those derived from ERA5 shows a good overall performance but also a clear large-scale spatial bias. Future research is needed to investigate the specific causes of the systemic errors and attempt to correct them. The projected changes for 2021-2050 using a strong warming scenario (SSP5-8.5) compared to 1951-1980 show that the 10-year surge level may see changes of up to -0.1 m or 20%. These changes are not uniform across the globe with, for example, a decrease in the Mediterranean Sea and an increase in Gulf of Carpentaria (Australia). Overall, the projected changes in storm surges are small compared to model bias, internal climate variability, and statistical uncertainties. We have outlined several future research directions that could be explored to further enhance the understanding of how extreme sea level will change in response to anthropogenic forcing.

Open research

The dataset underlying this analysis is openly available on the C3S Climate Data Store. It consists of timeseries of mean sea level, tides, storm surges and total water levels, as well as various water level statistics (i.e. percentiles, return periods, tidal levels). The timeseries can be found here: <https://cds-dev.copernicus-climate.eu/cdsapp#!/dataset/sis-water-level-change-timeseries-cmip6?tab=overview>, while the statistical indicators can be found here: <https://cds-dev.copernicus-climate.eu/cdsapp#!/dataset/sis-water-level-change-indicators-cmip6?tab=overview>. The ERA5 dataset was obtained from the Climate Data Store. The HighResMIP data archive can be accessed via ESGF server.

Acknowledgements

The research leading to these results received from the Deltares Strategic Research Program. SM and PJW received additional funding from the MOSAIC research program (ASDI.2018.036), which is financed by the Dutch Research Council (NWO). Additional work to make these results openly available was funded by Contract C3S-422-Lot2-Deltares European Services of the Copernicus Climate Change Service (11200665-003). PJW received additional funding received funding from the Dutch Research Council (NWO) in the form of a VIDI grant (grant no. 016.161.324). JAE received funding from ERC Advanced Grant project COASTMOVE (grant number 884442) and NWO VICI grant no. 453-13-006. RR was supported by the AXA Research Fund and the Deltares Natural Hazards Strategic Research Program. We acknowledge that the results of this research have been achieved using the DECI resource Cartesius based in The Netherlands at SURFsara with support from the PRACE aisbl. We thank Maxime Moge from SURFsara (<http://www.surfsara.nl>) for his support in using the Cartesius Computer Cluster. The authors also acknowledge Remco Plieger, Menno Genseberger, Robyn Gwee and Jelmer Veenstra for their contributions to this project. The CMIP6 HighResMIP datasets (available on the Earth System Grid Federation) were produced as part of the EU H2020 PRIMAVERA project (Grant Agreement 641727). MJR was supported by the Met Office Hadley Centre Climate Programme funded by BEIS and Defra (GA01101).

References

Bauer, P., Thorpe, A., & Brunet, G. (2015). The quiet revolution of numerical weather prediction. *Nature*. <https://doi.org/10.1038/nature14956> Bloemendaal, N., Muis, S., Haarsma, R. J., Verlaan, M., Moel, H. de, Ward, P. J., & Aerts, J. C. J. H. (2017). The effect of global atmospheric model spatial resolution on tropical cyclone surge representation. In *Presented at: 1st International Workshop on Waves, Storm Surges and Coastal Hazards, Liverpool, United Kingdom, 11-14 September 2017*. Liverpool, UK. Bouwer, L.

M. (2018). Next-generation coastal risk models. *Nature Climate Change*. <https://doi.org/10.1038/s41558-018-0262-2>

Calafat, F. M., Wahl, T., Tadesse, M. G., & Sparrow, S. N. (2022). Trends in Europe storm surge extremes match the rate of sea-level rise. *Nature* 2022 603:7903, 603(7903), 841–845. <https://doi.org/10.1038/s41586-022-04426-5>

Camargo, S. J. (2013). Global and regional aspects of tropical cyclone activity in the CMIP5 models. *Journal of Climate*. <https://doi.org/10.1175/JCLI-D-12-00549.1>

Charnock, H. (1955). Wind stress on a water surface. *Quart. J. Roy. Meteor. Soc.*, 81, 639–640.

Colberg, F., McInnes, K. L., O’Grady, J., & Hoeke, R. (2019). Atmospheric circulation changes and their impact on extreme sea levels around Australia. *Natural Hazards and Earth System Sciences*. <https://doi.org/10.5194/nhess-19-1067-2019>

Copernicus Climate Change Service (C3S). (2017). ERA5: Fifth generation of ECMWF atmospheric reanalyses of the global climate. Retrieved from <https://cds.climate.copernicus.eu/cdsapp#!/home>

Dullaart, J. C. M., Muis, S., Bloemendaal, N., & Aerts, J. C. J. H. (2020). Advancing global storm surge modelling using the new ERA5 climate reanalysis. *Climate Dynamics*, 54(1–2), 1007–1021. <https://doi.org/10.1007/s00382-019-05044-0>

Dullaart, J. C. M., Muis, S., Bloemendaal, N., Chertova, M. V., Couasnon, A., & Aerts, J. C. J. H. (2021). Accounting for tropical cyclones more than doubles the global population exposed to low-probability coastal flooding. *Communications Earth & Environment*, 2(1), 135. <https://doi.org/10.1038/s43247-021-00204-9>

EC-Earth Consortium. (2018). EC-Earth3P-HR model output prepared for CMIP6 HighResMIP. Version. Earth System Grid Federation. <https://doi.org/10.22033/ESGF/CMIP6.2323>

Eisner, S., Voss, F., & Kynast, E. (2012). Statistical bias correction of global climate projections - Consequences for large scale modeling of flood flows. *Advances in Geosciences*, 31, 75–82. <https://doi.org/10.5194/ADGEO-31-75-2012>

Fox-Kemper, B., Hewitt, H. T., Xiao, C., Aðalgeirsdóttir, G., Drijfhout, S. S., Edwards, T. L., et al. (2021). Ocean, Cryosphere and Sea Level Change. In V. Masson-Delmotte, P. Zhai, A. Pirani, S. L. Connors, C. Péan, S. Berger, et al. (Eds.), *Climate Change 2021: The Physical Science Basis. Contribution of Working Group I to the Sixth Assessment Report of the Intergovernmental Panel on Climate Change*. Cambridge University Press. <https://doi.org/10.5285/77B64C55-7166-4A06-9DEF-2E400398E452>

Frederikse, T., Buchanan, M. K., Lambert, E., Kopp, R. E., Oppenheimer, M., Rasmussen, D. J., & van de Wal, R. S. W. (2020). Antarctic Ice Sheet and emission scenario controls on 21st-century extreme sea-level changes. *Nature Communications*, 11(1), 390. <https://doi.org/10.1038/s41467-019-14049-6>

Garner, A. J., Mann, M. E., Emanuel, K. A., Kopp, R. E., Lin, N., Alley, R. B., et al. (2017). Impact of climate change on New York City’s coastal flood hazard: Increasing flood heights from the preindustrial to 2300 CE. *Proceedings of the National Academy of Sciences of the United States of America*, 114(45), 11861–11866. https://doi.org/10.1073/PNAS.1703568114/SUPPL_FILE/PNAS.201703568SI.PDF

Haarsma, R. J. (2021). European Windstorm Risk of Post-Tropical Cyclones and the Impact of Climate Change. *Geophysical Research Letters*, 48(4), e2020GL091483. <https://doi.org/10.1029/2020GL091483>

Haarsma, R. J., Hazeleger, W., Sever-

ijns, C., de Vries, H., Sterl, A., Bintanja, R., et al. (2013). More hurricanes to hit western Europe due to global warming. *Geophysical Research Letters*, 40(9), 1783–1788. <https://doi.org/10.1002/grl.50360>

Haarsma, R. J., Roberts, M. J., Vidale, P. L., Catherine, A., Bellucci, A., Bao, Q., et al. (2016). High Resolution Model Intercomparison Project (HighResMIP v1.0) for CMIP6. *Geoscientific Model Development*. <https://doi.org/10.5194/gmd-9-4185-2016>

Haigh, I. D., MacPherson, L. R., Mason, M. S., Wijeratne, E. M. S., Pattiaratchi, C. B., Crompton, R. P., & George, S. (2013). Estimating present day extreme water level exceedance probabilities around the coastline of Australia: tropical cyclone-induced storm surges. *Climate Dynamics*, 42(1–2), 139–157. <https://doi.org/10.1007/s00382-012-1653-0>

Hemer, M. A., Fan, Y., Mori, N., Semedo, A., & Wang, X. L. (2013). Projected changes in wave climate from a multi-model ensemble. *Nature Climate Change*, 3(5), 471–476. <https://doi.org/10.1038/nclimate1791>

Hersbach, H., Bell, B., Berrisford, P., Hirahara, S., Horányi, A., Muñoz-Sabater, J., et al. (2020). The ERA5 global reanalysis. *Quarterly Journal of the Royal Meteorological Society*. <https://doi.org/10.1002/qj.3803>

Hodges, K., Cobb, A., & Vidale, P. L. (2017). How well are tropical cyclones represented in reanalysis datasets? *Journal of Climate*. <https://doi.org/10.1175/JCLI-D-16-0557.1>

Irazoqui Apecechea, M., Verlaan, M., Williams, J., de Lima Rego, J., Muis, S., Kernkamp, H. W. J., et al. (2019). GTSM v3.0: A next generation Global Tide and Surge Model. *Ocean Dynamics, In Review*

Iturbide, M., Gutiérrez, J. M., Alves, L. M., Bedia, J., Cerezo-Mota, R., Cimadevilla, E., et al. (2020). An update of IPCC climate reference regions for subcontinental analysis of climate model data: definition and aggregated datasets. *Earth System Science Data*, 12(4), 2959–2970. <https://doi.org/10.5194/ESSD-12-2959-2020>

Kernkamp, H. W. J., Van Dam, A., Stelling, G. S., & de Goede, E. D. (2011). Efficient scheme for the shallow water equations on unstructured grids with application to the Continental Shelf. *Ocean Dynamics*, 61(8), 1175–1188. <https://doi.org/10.1007/s10236-011-0423-6>

Kirezci, E., Young, I. R., Ranasinghe, R., Muis, S., Nicholls, R. J., Lincke, D., & Hinkel, J. (2020). Projections of global-scale extreme sea levels and resulting episodic coastal flooding over the 21st Century. *Scientific Reports*. <https://doi.org/10.1038/s41598-020-67736-6>

Knutson, T. R., McBride, J. L., Chan, J., Emanuel, K. A., Holland, G. J., Landsea, C. W., et al. (2010). Tropical cyclones and climate change. *Nature Geoscience*, 3(3), 157–163. <https://doi.org/10.1038/ngeo779>

Knutson, T. R., Camargo, S. J., Chan, J. C. L., Emanuel, K., Ho, C. H., Kossin, J. P., et al. (2019). Tropical Cyclones and Climate Change Assessment: Part I: Detection and Attribution. *Bulletin of the American Meteorological Society*, 100(10), 1987–2007. <https://doi.org/10.1175/BAMS-D-18-0189.1>

Knutson, T. R., Camargo, S. J., Chan, J. C. L., Emanuel, K., Ho, C. H., Kossin, J. P., et al. (2020). Tropical Cyclones and Climate Change Assessment: Part II: Projected Response to Anthropogenic Warming. *Bulletin of the American Meteorological Society*, 101(3), E303–E322. <https://doi.org/10.1175/BAMS-D-18-0194.1>

Lemos, G., Menendez, M., Semedo, A., Camus, P., Hemer, M., Dobrynin, M., & Miranda, P. M. A. (2020). On the need of bias correc-

tion methods for wave climate projections. *Global and Planetary Change*. <https://doi.org/10.1016/j.gloplacha.2019.103109>Lin, N., & Emanuel, K. A. (2015). Grey swan tropical cyclones. *Nature Climate Change*, 6(August 2015), 106–112. <https://doi.org/10.1038/NCLIMATE2777>Lin, N., Marsooli, R., & Colle, B. A. (2019). Storm surge return levels induced by mid-to-late-twenty-first-century extratropical cyclones in the Northeastern United States. *Climatic Change*, 154(1–2), 143–158. <https://doi.org/10.1007/S10584-019-02431-8>/FIGURES/7Little, C. M., Horton, R. M., Kopp, R. E., Oppenheimer, M., Vecchi, G. A., & Villarini, G. (2015). Joint projections of US East Coast sea level and storm surge. *Nature Climate Change* 2015 5:12, 5(12), 1114–1120. <https://doi.org/10.1038/nclimate2801>Lockwood, J. W., Oppenheimer, M., Lin, N., Kopp, R. E., Vecchi, G. A., & Gori, A. (2022). Correlation Between Sea-Level Rise and Aspects of Future Tropical Cyclone Activity in CMIP6 Models. *Earth’s Future*, 10(4), e2021EF002462. <https://doi.org/10.1029/2021EF002462>Marcos, M., Rohmer, J., Vousdoukas, M. I., Mentaschi, L., Le Cozannet, G., & Amores, A. (2019). Increased Extreme Coastal Water Levels Due to the Combined Action of Storm Surges and Wind Waves. *Geophysical Research Letters*, 46(8), 4356–4364. <https://doi.org/10.1029/2019GL082599>Marsooli, R., Lin, N., Emanuel, K., & Feng, K. (2019). Climate change exacerbates hurricane flood hazards along US Atlantic and Gulf Coasts in spatially varying patterns. *Nature Communications*. <https://doi.org/10.1038/s41467-019-11755-z>Meucci, A., Young, I. R., Hemer, M., Kirezci, E., & Ranasinghe, R. (2020). Projected 21st century changes in extreme wind-wave events. *Science Advances*. <https://doi.org/10.1126/sciadv.aaz7295>Mori, N., Shimura, T., Yoshida, K., Mizuta, R., Okada, Y., Fujita, M., et al. (2019). Future changes in extreme storm surges based on mega-ensemble projection using 60-km resolution atmospheric global circulation model. *Coastal Engineering Journal*. <https://doi.org/10.1080/21664250.2019.1586290>Morim, J., Hemer, M., Wang, X. L., Cartwright, N., Trenham, C., Semedo, A., et al. (2019). Robustness and uncertainties in global multivariate wind-wave climate projections. *Nature Climate Change* 2019 9:9, 9(9), 711–718. <https://doi.org/10.1038/s41558-019-0542-5>Muis, S., Verlaan, M., Winsemius, H. C., Aerts, J. C. J. H., & Ward, P. J. (2016). A global reanalysis of storm surges and extreme sea levels. *Nature Communications*, 7(7:11969), 1–11. <https://doi.org/10.1038/ncomms11969>Muis, S., Lin, N., Verlaan, M., Winsemius, H. C., Ward, P. J., & Aerts, J. C. J. H. (2019). Spatiotemporal patterns of extreme sea levels along the western North-Atlantic coasts. *Scientific Reports*, 9(1). <https://doi.org/10.1038/s41598-019-40157-w>Muis, S., Apecechea, M. I., Dullaart, J., de Lima Rego, J., Madsen, K. S., Su, J., et al. (2020). A High-Resolution Global Dataset of Extreme Sea Levels, Tides, and Storm Surges, Including Future Projections. *Frontiers in Marine Science*, 7. <https://doi.org/10.3389/fmars.2020.00263>Murakami, H., Wang, Y., Yoshimura, H., Mizuta, R., Sugi, M., Shindo, E., et al. (2012). Future changes in tropical cyclone activity projected by the new high-resolution MRI-AGCM. *Journal of Climate*. <https://doi.org/10.1175/JCLI-D-11-00415.1>Navarro-Racines, C., Tarapues, J., Thornton, P., Jarvis, A., & Ramirez-Villegas,

J. (2020). High-resolution and bias-corrected CMIP5 projections for climate change impact assessments. *Scientific Data* 2020 7:1, 7(1), 1–14. <https://doi.org/10.1038/S41597-019-0343-8>

Neill, B. C., Tebaldi, C., Van Vuuren, D. P., Eyring, V., Friedlingstein, P., Hurtt, G., et al. (2016). The Scenario Model Intercomparison Project (ScenarioMIP) for CMIP6. *Geoscientific Model Development*, 9(9), 3461–3482. <https://doi.org/10.5194/GMD-9-3461-2016>

Orton, P. M., Hall, T. M., Talke, S. A., Blumberg, A., Georgas, N., & Vinogradov, S. (2016). A validated tropical-extratropical flood hazard assessment for New York Harbor. *Journal of Geophysical Research: Oceans*, 121, 8904– 8929. <https://doi.org/10.1002/2016JC011679>

Powell, M. D., Vickery, P. J., & Reinhold, T. A. (2003). Reduced drag coefficient for high wind speeds in tropical cyclones. *Nature*, 422(6929), 279–283. <https://doi.org/10.1038/nature01481>

Priestley, M. D. K., Ackerley, D., Catto, J. L., & Hodges, K. I. (2022). Drivers of biases in the CMIP6 extratropical storm tracks. Part 1: Northern Hemisphere. *Journal of Climate*, 1(aop), 1–37. <https://doi.org/10.1175/JCLI-D-20-0976.1>

Rasmussen, D. J., Bittermann, K., Buchanan, M. K., Kulp, S., Strauss, B. H., Kopp, R. E., & Oppenheimer, M. (2018). Extreme sea level implications of 1.5 °C, 2.0 °C, and 2.5 °C temperature stabilization targets in the 21st and 22nd centuries. *Environmental Research Letters*, 13(3), 034040. <https://doi.org/10.1088/1748-9326/AAAC87>

Ridder, N., de Vries, H., Drijfhout, S., van den Brink, H. W., van Meijgaard, E., & de Vries, H. (2018). Extreme storm surge modelling in the North Sea: The role of the sea state, forcing frequency and spatial forcing resolution. *Ocean Dynamics*, 68(2), 255–272. <https://doi.org/10.1007/s10236-018-1133-0>

Roberts, M. (2017). MOHC HadGEM3-GC31-HM model output prepared for CMIP6 HighResMIP. Earth System Grid Federation. <https://doi.org/10.22033/ESGF/CMIP6.446>

Roberts, M. J., Camp, J., Seddon, J., Vidale, P. L., Hodges, K., Vanniere, B., et al. (2020). Impact of model resolution on tropical cyclone simulation using the HighResMIP-PRIMAVERA multimodel ensemble. *Journal of Climate*. <https://doi.org/10.1175/JCLI-D-19-0639.1>

Schenkel, B. A., & Hart, R. E. (2012). An examination of tropical cyclone position, intensity, and intensity life cycle within atmospheric reanalysis datasets. *Journal of Climate*, 25(10), 3453–3475. <https://doi.org/10.1175/2011JCLI4208.1>

Scoccimarro, E., Bellucci, A., & Peano, D. (2017). CMIP6 Citation “CMCC CMCC-CM2-VHR4 model output prepared for CMIP6 HighResMIP.” Earth System Grid Federation. <https://doi.org/10.22033/ESGF/CMIP6.1367>

Seneviratne, S. I., Zhang, X., Adnan, M., Badi, W., Dereczynski, C., Luca, A. Di, et al. (2021). Weather and Climate Extreme Events in a Changing Climate. In R. Y. and B. Z. Masson-Delmotte, V., P. Zhai, A. Pirani, S. L. Connors, C. Péan, S. Berger, N. Caud, Y. Chen, L. Goldfarb, M. I. Gomis, M. Huang, K. Leitzell, E. Lonnoy, J. B. R. Matthews, T. K. Maycock, T. Waterfield, O. Yelekçi, R. Yu and B. Zhou Masson-Delmotte, V., P. (Ed.), *Climate Change 2021: The Physical Science Basis. Contribution of Working Group I to the Sixth Assessment Report of the Intergovernmental Panel on Climate Change* (In Press). Cambridge University Press.

Sobel, A. H., Wing, A. A., Camargo, S. J., Patricola, C. M., Vecchi,

G. A., Lee, C.-Y., & Tippett, M. K. (2021). Tropical cyclone frequency. *Earth's Future*, e2021EF002275. <https://doi.org/10.1029/2021EF002275>

Tebaldi, C., & Knutti, R. (2007). The use of the multi-model ensemble in probabilistic climate projections. *Phil. Trans. R. Soc. A*, 365(1857), 2053–75. <https://doi.org/10.1098/rsta.2007.2076>

Tebaldi, C., Ranasinghe, R., Vourdoukas, M. I., Rasmussen, D. J., Vega-Westhoff, B., Kirezci, E., et al. (2021). Extreme sea levels at different global warming levels. *Nature Climate Change* 2021 11:9, 11(9), 746–751. <https://doi.org/10.1038/s41558-021-01127-1>

Tiggeloven, T., De Moel, H., Winsemius, H. C., Eilander, D., Erkens, G., Gebremedhin, E., et al. (2020). Global-scale benefit-cost analysis of coastal flood adaptation to different flood risk drivers using structural measures. *Natural Hazards and Earth System Sciences*. <https://doi.org/10.5194/nhess-20-1025-2020>

Vitousek, S., Barnard, P. L., Fletcher, C. H., Frazer, N., Erikson, L., & Storlazzi, C. D. (2017). Doubling of coastal flooding frequency within decades due to sea-level rise. *Scientific Reports*, 7(1), 1399. <https://doi.org/10.1038/s41598-017-01362-7>

Vourdoukas, M. I., Voukouvalas, E., Annunziato, A., Giardino, A., & Feyen, L. (2016). Projections of extreme storm surge levels along Europe. *Climate Dynamics*, 47(9), 1–20. <https://doi.org/10.1007/s00382-016-3019-5>

Vourdoukas, M. I., Mentaschi, L., Voukouvalas, E., Verlaan, M., Jevrejeva, S., Jackson, L. P., & Feyen, L. (2018). Global probabilistic projections of extreme sea levels show intensification of coastal flood hazard. *Nature Communications*. <https://doi.org/10.1038/s41467-018-04692-w>

Wahl, T. (2017). Sea-level rise and storm surges, relationship status: complicated! *Environmental Research Letters*, 12(11), 111001. <https://doi.org/10.1088/1748-9326/aa8eba>

Wahl, T., Haigh, I. D., Nicholls, R. J., Arns, A., Dangendorf, S., Hinkel, J., & Slangen, A. (2017). Understanding extreme sea levels for broad-scale coastal impact and adaptation analysis. *Nature Communications*, 8, 16075. <https://doi.org/10.1038/ncomms16075>

Walsh, K. J. E., McBride, J. L., Klotzbach, P. J., Balachandran, S., Camargo, S. J., Holland, G., et al. (2016). Tropical cyclones and climate change. *Wiley Interdisciplinary Reviews: Climate Change*. <https://doi.org/10.1002/wcc.371>

Wang, X., Verlaan, M., Apecechea Irazoqui, M., & Lin, H. X. (2021). Computation-Efficient Parameter Estimation for a High-Resolution Global Tide and Surge Model. *Journal of Geophysical Research: Oceans*. <https://doi.org/10.1029/2020jc016917>

Wilcox, R. R. (2010). The Bootstrap. In *Fundamentals of Modern Statistical Methods* (pp. 87–108). New York, NY: Springer New York. https://doi.org/10.1007/978-1-4419-5525-8_6

Woodworth, P. L., Melet, A., Marcos, M., Ray, R. D., Wöppelmann, G., Sasaki, Y. N., et al. (2019). Forcing Factors Affecting Sea Level Changes at the Coast. *Surveys in Geophysics*. <https://doi.org/10.1007/s10712-019-09531-1>

Zhao, M., Blanton, C., John, J. G., Radhakrishnan, A., Zadeh, N. T., McHugh, C., et al. (2018). NOAA-GFDL GFDL-CM4C192 model output prepared for CMIP6 HighResMIP highresSST-present. Earth System Grid Federation. <https://doi.org/10.22033/ESGF/CMIP6.8565>